

The double AGN in NGC 6240 revealed through 3-5 μm spectroscopy*

G. Risaliti^{1,2}, E. Sani³, R. Maiolino¹, A. Marconi¹, S. Berta⁴, V. Braitto⁵, R. Della Ceca⁵,
A. Franceschini⁴, M. Salvati¹

grisaliti@cfa.harvard.edu

ABSTRACT

We present 3-5 μm spectroscopy of the interacting system NGC 6240, showing the presence of two active galactic nuclei. The brightest (southern) nucleus shows up with a starburst-like emission, with a prominent 3.3 μm emission feature. However, the presence of an AGN is revealed by the detection of a broad Br α emission line, with a width of $\sim 1,800 \text{ km s}^{-1}$. The spectrum of the faintest (northern) nucleus shows typical AGN features, such as a steep continuum and broad absorption features in the M-band.

We discuss the physical properties of the dusty absorbers/emitters, and show that in both nuclei the AGN is dominant in the 3-5 μm band, but its contribution to the total luminosity is small (a few percent of the starburst emission).

Subject headings: Galaxies: active — Infrared: galaxies — Galaxies: individual (NGC 6240)

1. Introduction

L-band spectroscopy ($\sim 3 - 4 \mu\text{m}$) of Ultraluminous Infrared Galaxies (ULIRGs) is a powerful tool to disentangle the starburst and AGN contributions to the huge ($> 10^{12} L_{\odot}$)

*Based on observations collected at the European Southern Observatory, Chile (proposal 73.B-0574)

¹INAF - Osservatorio di Arcetri, L.go E. Fermi 5, Firenze, Italy

²Harvard-Smithsonian Center for Astrophysics, 60 Garden St. Cambridge, MA 02138 USA

³Dipartimento di Astronomia, Università di Firenze, L.go E. Fermi 2, I-50125 Firenze, Italy

⁴Dipartimento di Astronomia, Università di Padova, Italy

⁵ INAF - Osservatorio Astronomico di Brera, Milano, Italy

infrared luminosity. Several spectral features can be used as indicators of one of the two components (e.g. Imanishi & Dudley 2000, Risaliti et al. 2005, hereafter R05). More specifically:

- a large equivalent width of the 3.3 μm PAH emission feature ($EW_{3.3} \sim 100$ nm) is typical of starburst-dominated sources;
- a strong absorption feature at 3.4 μm ($\tau_{3.4} > 0.2$), due to aliphatic hydrocarbon grains, is an indicator of an obscured AGN;
- a steep red continuum ($f_\lambda \propto \lambda^\Gamma, \Gamma > 2$) suggests the presence of an obscured, reddened AGN.

M-band spectra (4.5–5 μm) of ULIRGs are available only for a small number of sources. From the analysis of the M-band emission of the nearby obscured AGN NGC 4945 (Spoon et al. 2003) strong absorption features due to CO ices are expected for obscured AGNs.

NGC 6240 is an interacting system consisting of two nuclei with a separation of 1.8 arcsec (Fried & Schulz 1984), corresponding to ~ 800 pc¹ and with a total infrared luminosity $L_{IR} = 10^{11.8} L_\odot$ (Genzel et al. 1998). It is optically classified as a LINER (Rafanelli et al. 1997), and no indications of an AGN, such as broad Pa α or Br γ lines, are present in the near-IR. L-band spectroscopy, performed with a four meter class telescope, did not resolve the two nuclei, and showed a typical starburst emission, with a flat continuum, a strong 3.3 μm emission feature ($EW \sim 70$ nm), and no absorption features (Imanishi & Dudley 2000). In the hard X-rays the AGN emission is dominant above 10 keV (Vignati et al. 1999), while at lower energy only the reflected component is visible, due to the high column density ($N_H \sim 2 \times 10^{24}$ cm⁻²) obscuring the direct component. In a recent *Chandra* observation the two nuclei are clearly separated, and both show a prominent iron $K\alpha$ emission line, with $EW > 1$ keV, indicating the presence of an AGN in both nuclei (Komossa et al. 2003). This is the first clear detection of a double AGN in an interacting system.

Here we present new VLT L-band and M-band spectra of the two nuclei of NGC 6240, both showing clear AGN features.

2. Reduction and Data Analysis

NGC 6240 was observed with the Infrared Spectrometer And Array Camera (ISAAC) at the Antu Unit (UT1) of the Very Large Telescope on Cerro Paranal, Chile, on July 31, 2005, with photometric conditions and a seeing of 0.6 arcsec in the infrared. We performed the

¹We adopt $H_0 = 70$ km s⁻¹ Mpc⁻¹, e.g. Spergel et al. 2003).

observations in low resolution mode, with the L-band (2.9-4.2 μm) and M-band (4.2-5.1 μm) filters, with a 0.6x20 arcsec slit, oriented in order to obtain spectra of both nuclei. The spectral resolution was $\lambda/\Delta\lambda \sim 600$ in the L-band and $\lambda/\Delta\lambda \sim 800$ in the M-band. The on-source observation times are 45 min in the L-band and 60 min in the M-band.

In order to avoid saturation due to the high background (~ 3.9 mag per arcsec² in L-band; ~ 1.2 mag in the M-band) the spectra were taken in chopping mode, with single exposures of 0.56 s. The spectra were then aligned and merged into a single image. We performed a standard data reduction, consisting of flat-fielding, background subtraction, and spectrum extraction, using the IRAF 2.11 package. In order to facilitate the background subtraction, the observations were performed by nodding the source along the slit (with a throw of 20 arcsec) Both nuclei are unresolved, but the tail of their emissions overlap. In particular, the contribution of the brightest nucleus to the emission in the extraction region of the faint nucleus is not negligible. In order to correct for this contamination, we subtracted from the faint nucleus a background extracted from the region symmetric to the extraction region with respect to the emission peak of the bright nucleus (Fig. 1).

We acquired the spectra of the standard star (HR 5249, spectral type B2V) immediately after the target observations. Corrections for sky absorption and instrumental response were obtained from the spectra of the standard star, divided by its intrinsic emission, assumed to be a pure Rayleigh-Jeans spectrum.

In order to obtain a precise absolute calibration, we took into account aperture effects by analyzing the profiles of both the targets and the standard stars along the slit. We assumed a Gaussian profile and we estimated the fraction of flux inside the slit assuming a perfect centering. We estimate this procedure to have an error $< 10\%$ for the L-band and $< 20\%$ for the M-band. The precision of the absolute calibration is confirmed by (a) the agreement within 10% with the L-band spectrum of Imanishi & Dudley (2000), and (b) the cross calibration between our L-band and M-band spectra, which match within 15%.

The atmospheric transmission is not constant in the 3-5 μm range. In several narrow spectral intervals in the M-band, and one in the L-band, the transparency is too low to obtain significant data. We excluded these intervals from our spectral analysis. In other wavelength ranges, such as between 2.9 and 3.2 μm , and in the M-band in general, the atmospheric conditions vary in short timescales. This implies that the sky features are not completely removed with the division by the calibration star. We rebinned the spectral channels in these intervals in order to have significant spectral points. Finally, for the spectral intervals with good atmospheric transmission and high signal-to-noise (such as the brightest nucleus in the 3.4-4.1 μm interval) we chose the rebinning in order to have a spectral element covering a wavelength interval of $\sim 30 \text{ \AA}$, a factor 2 smaller than the spectral resolution.

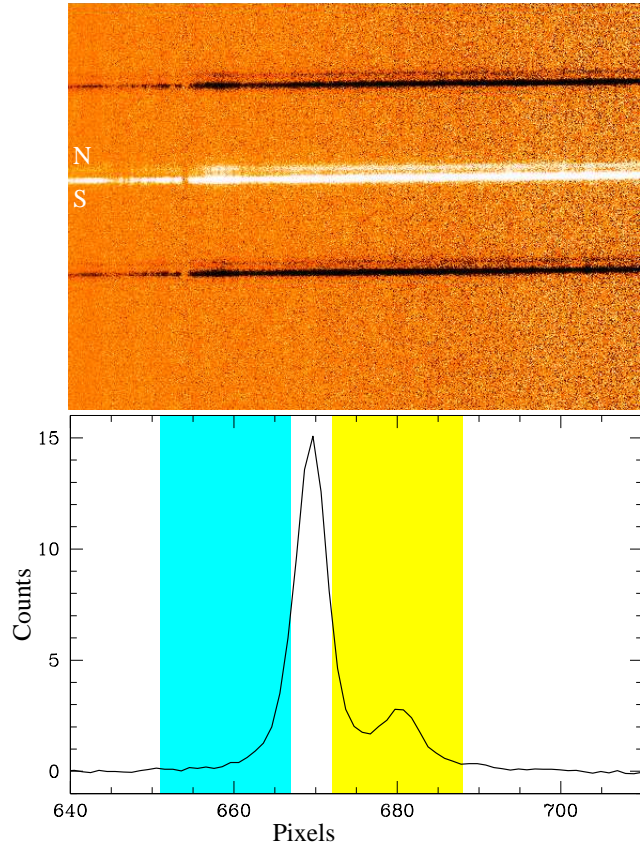


Fig. 1.— Upper panel: L-band spectrum of NGC 6240. The 2 nuclei are clearly separated. Lower panel: Integrated emission along the slit. We extracted the spectrum of the faintest nucleus from the cyan shaded region on the right. The background was extracted from the yellow shaded region on the left, symmetric with the source region with respect to the emission peak of the brightest nucleus.

We fitted the spectra with a power law continuum and broad Gaussian absorption and emission lines. We left the relative normalizations between the L and M bands free to vary within the uncertainties given above. The results are shown in Fig. 2.

2.1. NGC 6240S

The 3-5 μm spectral properties of the brightest, southern nucleus are the following:

- A flat $\lambda - f_\lambda$ continuum, with a slope ($\Gamma(S) = -0.3 \pm 0.1$) typical of both starbursts and unobscured AGNs (R05).
- An emission feature at 3.3 μm , with $EW_{3.3}(S) = 49 \pm 5$ nm, a factor ~ 2 smaller than in pure starbursts (Imanishi & Dudley 2000, R05), thus indicating the presence of an AGN.
- A broad Br α line at 4.05 μm (rest frame) with a full width at half maximum corresponding to a velocity of $1,800 \pm 200$ km s $^{-1}$. This is a clear, direct evidence of the presence of an AGN in this nucleus. The Pf β line at 4.65 μm is also detected, but the possible atmospheric turbulence and CO absorption bands prevent us from analyzing the main line properties, such as profile and equivalent width.
- A 3.1 μm ice absorption feature, with $\tau_{3.1}(S) = 0.2 \pm 0.05$, and no clear absorption features at 3.4 μm .
- Possible absorption features due to CO ice in the 4.5-4.8 μm range. The strength of these features depends on the assumed continuum level. Given the concave shape of the spectrum, and that no strong emission feature is known around 4.6 μm , we chose the normalization of the M-band spectrum in order to obtain a good match between the extrapolation of the L-band continuum and the highest points in the 4.5-4.6 μm interval. The above analysis clearly indicates the presence of both an AGN and a starburst as sources of the 3-5 μm emission.

2.2. NGC 6240N

The fainter, northern nucleus also shows a 3-5 μm emission with clear contributions from both an AGN and a starburst:

- The continuum is rather steep ($\Gamma(N) = 1.5 \pm 0.1$). Such a steepness is not typical either of starburst-dominated sources nor of unobscured AGNs, and is observed only in objects hosting a heavily obscured, reddened AGN (R05).
- The PAH emission feature at 3.3 μm is present, with $EW(N) = 48 \pm 3$ nm, a factor of 2 smaller than in starburst-dominated sources, clearly indicating the presence of a starburst, diluted by an AGN component.

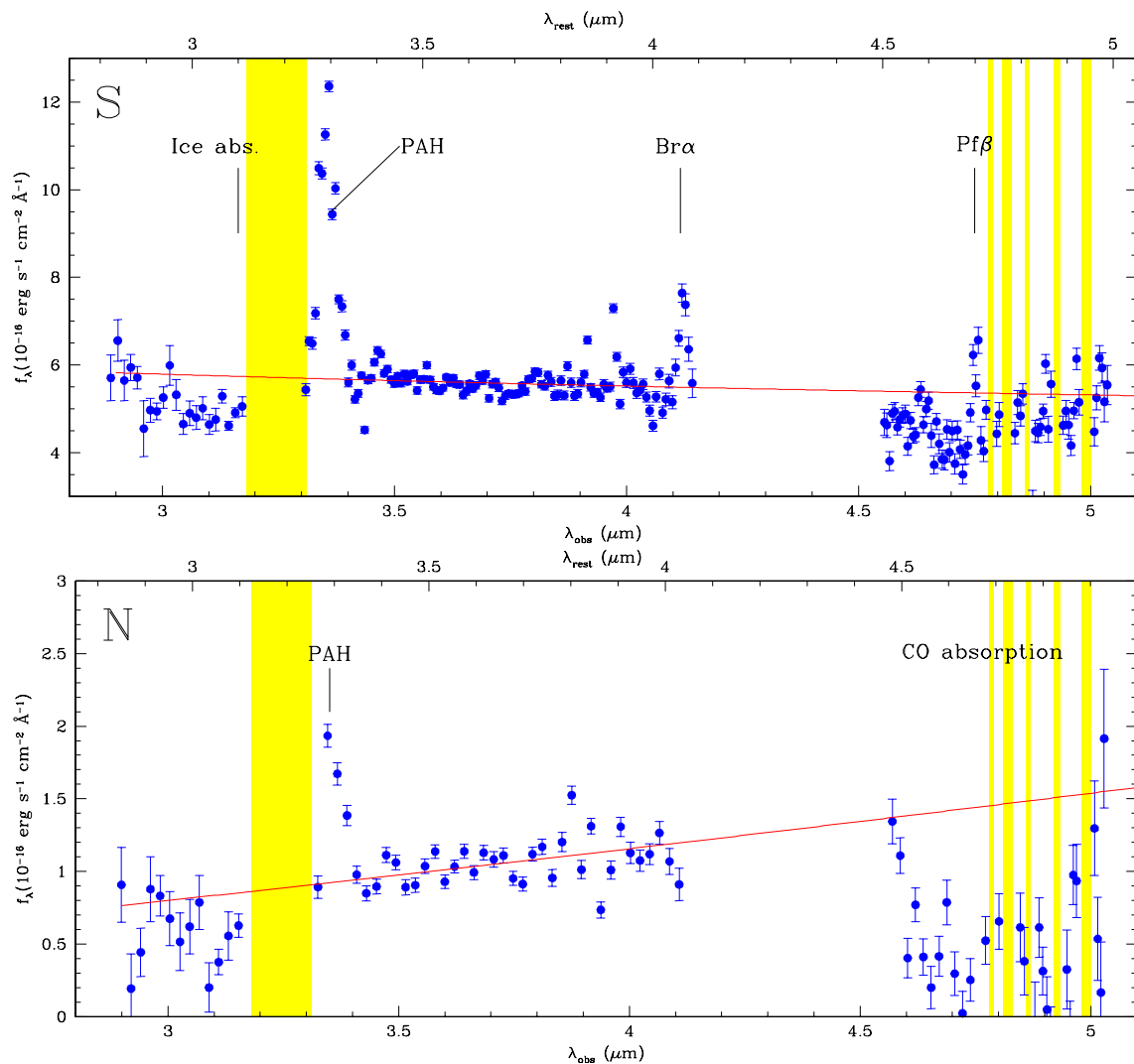


Fig. 2.— Complete L-band and M-band spectra of the two nuclei of NGC 6240. We rescaled the M-band spectra in order to match the normalization of the L-band spectrum (see text for details). The yellow shaded regions show the wavelength intervals with bad atmospheric transmission. The main spectral features are labeled.

- The M-band spectrum can be interpreted as dominated by deep absorption features due to CO ice. Again, this interpretation is not unique, due to the uncertainty on the continuum level. However, if the continuum is assumed to be lower (so decreasing the strength of the absorption features) a strong emission feature at $4.6 \mu\text{m}$ would emerge, with no obvious explanation.

3. Discussion

We have shown that both AGN and starburst components are required to explain the 3-5 micron emission from both nuclei of NGC 6240. Here we quantitatively estimate the relative contribution of the two nuclei to the L-band and bolometric luminosities of the source, and we discuss the physical conditions of the dusty absorber/emitter.

1. Relative AGN/starburst contributions. In order to estimate the relative contribution of the AGN to the 3-5 μm emission in the two nuclei, we use a simple model to disentangle the two components, as shown in R05. We assume that the intrinsic spectrum of the AGN, $f_\lambda(\text{AGN})$, is a power law with a spectral index $\Gamma = -0.5$, in agreement with the L-band spectra of ULIRGs dominated by unabsorbed AGNs (R05). The observed AGN spectrum is obtained from the intrinsic spectrum, absorbed by a wavelength-dependent optical depth, $\tau(\lambda) \propto \lambda^{-1.75}$ (Cardelli et al. 1989). The starburst component $f_\lambda(\text{SB})$, is modelled by a continuum with $\Gamma = -0.5$ (as for unobscured AGNs) plus a broad emission feature at $3.3 \mu\text{m}$ having $\text{EW}_{3.3}=100 \text{ nm}$. This is in agreement with the average observed L-band spectra of starburst-dominated ULIRGs (Imanishi & Dudley 2000, R05). The ULIRG emission, f_λ , is obtained as the combination of the two components:

$$f_\lambda = \alpha f_\lambda(\text{AGN})e^{-\tau(\lambda)} + (1 - \alpha)f_\lambda(\text{SB}) \quad (1)$$

where α is the fraction of the *intrinsic* L-band luminosity due to the AGN. We express the optical depth as $\tau(\lambda) = \tau_L \times (\lambda/3.5\mu\text{m})^{-1.75}$, where τ_L is the optical depth at $3.5 \mu\text{m}$. Therefore, the model has two free parameters, α and τ_L . From the composite spectrum, the equivalent width of the $3.3 \mu\text{m}$ feature and the continuum slope can be computed as a function of the above parameters. Therefore, we can find the unique solution for τ_L and α which reproduces the observed values of $\text{EW}_{3.3}$ and Γ . We obtain $\tau_L(S) = 0.6 \pm 0.2$, $\alpha(S) = 0.6 \pm 0.1$, and $\tau_L(N) = 2.0 \pm 0.2$, $\alpha(N) = 0.9 \pm 0.03$. The quoted errors are based on the measured errors on $\text{EW}_{3.3}$ and Γ . An additional source of systematic errors could be the uncertainty on the intrinsic AGN and SB spectral slope, and on the intrinsic EW in SBs. If

these are taken into account, our errors could be larger by a factor $\sim 2^2$.

In order to estimate the relative AGN/SB contribution to the bolometric luminosity, we need to take into account the ratio, K , between the contribution of the L-band emission to the bolometric luminosity in a pure AGN and that in a pure starburst. From the average L-band to bolometric ratio in pure starbursts ($\sim 2 \times 10^{-3}$, R05) and in quasars (~ 0.2 , from the spectral energy distribution of Elvis et al. 1994), we obtain $K \sim 100$. The contributions of the AGN component to the bolometric luminosity,

$$\alpha_{BOL} = \alpha / (\alpha + K(1 - \alpha)) \quad (2)$$

are then $\alpha_{BOL}(S) = 2 \pm 0.5\%$ and $\alpha_{BOL}(N) = 10 \pm 2\%$. The uncertainty on K can be as large as a factor of 3-5. However, it is easily seen from Eq. 2 that this does not affect our main conclusion, which is $\alpha_{BOL} \ll 1$, provided that $K \gg 1$.

Summarizing, the interesting result which emerges from the above analysis is that a moderately absorbed AGN is present in both sources, with a dominant contribution to the L-band emission, but a minor contribution to the bolometric luminosity.

2. Physical properties of the dusty emitter/absorber. The above analysis suggests a moderate L-band absorption of the AGN component in both nuclei. Assuming a standard extinction curve ($A_V \sim 25 A_L$, Cardelli, Clayton & Mathis 1989) we have $A_V(S) \sim 15$ and $A_V(N) \sim 50$. This is in agreement with the estimates of Lutz et al. (2003) based on the mid-IR spectrum of both nuclei (and, therefore, dominated by the emission of the S nucleus), and with the absence of other broad lines in the optical and near-IR spectra, which suffer high extinction and dilution by the starburst component. Instead, the Br α line is obscured by only $\tau(S) \sim 0.6$, and lies in a spectral region where the AGN emission is dominant. This makes Br α an excellent atomic emission line to discover obscured AGN, as first noticed by Lutz et al. (2000).

More in general, we note that in sources such as NGC 6240, where the AGN is obscured by $A_V > 20$, $N_H > 10^{24} \text{ cm}^{-2}$, and the starburst dominates the bolometric emission, the AGN emission is dominant in two spectral windows only: the infrared region between 3 and 5-8 μm , and the hard X-ray region, at $E > 10 \text{ keV}$. In the whole wavelength range between the L-band and the hard X-rays the AGN is completely obscured, while in the mid and far infrared its emission is strongly diluted by the starburst component.

The estimated values for the extinction are smaller by a factor about 50 than the value expected from the X-ray spectra, $A_V \sim 1000$, if a Galactic dust-to-gas ratio is assumed

²For further details on this model and on errors estimates, we refer to R05, where the model is also applied to a larger sample of ULIRGs.

($A_V/N_H = 1.7 \times 10^{21} \text{ mag}^{-1} \text{ cm}^2$, Bohlin, Savage & Drake 1978). This discrepancy can be explained in two ways:

a) a lower than Galactic dust-to-gas ratio. This is commonly found in Seyfert galaxies (Maccacaro, Elvis & Perola 1984, Maiolino et al. 2001) and is probably common also among higher redshift quasars (Risaliti & Elvis 2005). The low ratio can be due either to the presence of a dust-free region of gas (this is expected if part of the absorbing gas lies within the dust sublimation radius) or to dust grains with on-average larger sizes than in the Galaxy (Maiolino, Marconi & Oliva 2002)

b) The amount of absorbing gas/dust towards the X-ray emitting region could be higher than towards the more extended L-band emitting region. The X-rays are expected to be emitted within a few tens of Schwarzschild radii from the central black hole of the AGN, i.e. within $\sim 10^{-2}$ parsec for a $10^8 M_\odot$ black hole, while the hot dust region must be at a distance R larger than the sublimation radius (for an AGN with an intrinsic optical/UV luminosity of $10^{46} \text{ erg s}^{-1}$, $R > 1$ parsec).

4. Conclusions

We have presented 3-5 μm low resolution spectra of the two nuclei in the Ultraluminous Infrared Galaxy NGC 6240, showing clear evidence of the presence of an AGN in both nuclei. This confirms the early detection of the double AGN obtained in the hard X-rays with *Chandra* (Komossa et al. 2003).

In the southern, brighter nucleus a broad Br α emission line is detected, the only known BLR evidence in the spectrum of this source.

The northern nucleus shows a steep L and M band emission, typical of a reddened ($\tau_L \sim 2$) AGN, with possible strong CO absorption features in the M-band.

In both nuclei the AGN emission dominates in the 3-5 μm band, but its contribution to the bolometric luminosity is small. The nuclear activity in sources like NGC 6240, i.e. where the AGN is faint (compared to the starburst) and obscured, is non-negligible only in the infrared between 3 and $\sim 5 - 8 \mu\text{m}$ and in the hard X-rays. At other wavelength the AGN is either obscured or strongly diluted by the starburst emission.

REFERENCES

Bohlin, R. C., Savage, B. D., & Drake, J. F. 1978, ApJ, 224, 132

- Cardelli, J. A., Clayton, G. C., & Mathis, J. S. 1989, *ApJ*, 345, 245
- Elvis, M., et al. 1994, *ApJS*, 95, 1
- Fried, J. W., & Schulz, H. 1983, *A&A*, 118, 166
- Genzel, R., et al. 1998, *ApJ*, 498, 579
- Imanishi, M., & Dudley, C. C. 2000, *ApJ*, 545, 701
- Komossa, S., Burwitz, V., Hasinger, G., Predehl, P., Kaastra, J. S., & Ikebe, Y. 2003, *ApJ*, 582, L15
- Lutz, D., et al. 2000, *ApJ*, 530, 733
- Lutz, D., Sturm, E., Genzel, R., Spoon, H. W. W., Moorwood, A. F. M., Netzer, H., & Sternberg, A. 2003, *A&A*, 409, 867
- Maccacaro, T., Perola, G. C., & Elvis, M. 1982, *ApJ*, 257, 47
- Maiolino, R., Marconi, A., Salvati, M., Risaliti, G., Severgnini, P., Oliva, E., La Franca, F., & Vanzi, L. 2001, *A&A*, 365, 28
- Maiolino, R., Marconi, A., & Oliva, E. 2001, *A&A*, 365, 37
- Rafanelli, P., Schulz, H., Barbieri, C., Komossa, S., Mebold, U., Baruffolo, A., & Radovich, M. 1997, *A&A*, 327, 901
- Risaliti, G., et al. 2005, *MNRAS*, accepted (R05, astro-ph/0510861)
- Risaliti, G., & Elvis, M. 2005, *ApJ*, 629, L17
- Spergel, D. N., et al. 2003, *ApJS*, 148, 175
- Spoon, H. W. W., Moorwood, A. F. M., Pontoppidan, K. M., Cami, J., Kregel, M., Lutz, D., & Tielens, A. G. G. M. 2003, *A&A*, 402, 499
- Vignati, P., et al. 1999, *A&A*, 349, L57